International Journal of Nanoelectronics and Materials
Volume 16, No. 4, October 2023 [737-748]

Tailoring the Structural and Optical Properties of Oxychloride Magnesium Tellurite Glass with the Addition of Samarium Ions

Nurul Ainaa Najihah Busra[1], Harizah Nadzmi[1], Rodziah Nazlan[1,*]

[1]Faculty of Industrial Sciences and Technology, Universiti Malaysia Pahang, Lebuh Persiaran Tun Khalil Yaakob 26300, Kuantan Pahang, Malaysia

Received 11 January 2023, Revised 11 April 2023, Accepted 17 July 2023

ABSTRACT

In this study, samarium-doped oxychloride magnesium tellurite glass with composition (79–x)TeO_2–xMgO–20Li_2O–1Sm_2O_3 (Series 1) and (79–x)TeO_2x$MgCl_2$–20Li_2O–1Sm_2O_3 (Series 2) with 0 ≤ x ≤ 15 mol% was prepared by the melt-quenching technique. The structural and optical properties of synthesized samples were investigated, and the XRD results dictated an amorphous nature for both samples. The glass density of both Series 1 and 2 decreased with increasing MgO and $MgCl_2$ content. However, the molar volume behaves in a completely opposite manner to an increase in MgO or $MgCl_2$ content. FTIR spectra revealed from the vibrational wavenumber shift of TeO^4 and TeO^3 structural units showed a significant rise in HOH vibration mode, which implies its usefulness in boosting water and light absorption. Four absorbance bands were observed via UV-Vis NIR, while the indirect optical band gap around (3.42–3.36) eV and (3.42–3.30) eV for Series 1 and Series 2 were observed from UV-Vis spectroscopy. The emission spectra from the photoluminescence study revealed four distinct bands centered at 562.54, 599.14, 645.63 and 708.40 nm which are attributed to the transition from $^4G_{5/2} - {}^6H_{J/2}$ (J = 5,7,9,11) of states of Sm^{3+}. The optimum glass with a composition of TeO-MgO 15% demonstrates a high potential for optical device development.

Keywords: Indirect optical band gap, Oxychloride magnesium, Tellurite glass, UV-Vis spectroscopy

1. INTRODUCTION

Tellurite-based glasses have piqued the interest among several researchers in recent years due to their intriguing mechanical, physical, and chemical properties. Müller discovered tellurium (Te) while working in Hungarian gold mines in 1782. In light transmission, tellurite color varies from white to yellow, and bright yellow to orange yellow [1]. Tellurium dioxide (TeO_2) is a solid oxide tellurium that exists in two forms: the yellow orthorhombic mineral tellurite, α-TeO_2, and the synthetic, colourless tetragonal (paratellurite), β-TeO_2 [2].

Tellurite glass has a higher refractive index, low melting temperature, low photon energy, high dielectric constant, and improved rare earth ion solubility in contrast to other glass systems such as fluoride glasses, borate glasses, and silicate glasses [3]. Tellurite glasses may also be used to make fibre, planar broadband amplifiers, and lasers [4]. However, TeO_2 glass has weak glass network connectivity, which makes it unstable. The durable, heat-resistant, and high electrical resistivity glasses can be improvised or altered into better and more precise properties to meet criteria for different applications. The addition of a small amount of modifier can transform glass

* Corresponding author: rodziah@ump.edu.my

into a wonder material. These include an alkaline earth metal oxide; magnesia (MgO), calcium oxide (CaO), strontia (SrO), and baria (BaO).

The loosely bonded atoms between the oxygen cause the glass modifier to disrupt the natural bonding between the glass-forming elements and oxygen, which results in significant effects such as a lower melting point, high chemical durability, and resistivity [5]. The unique physical properties and optical properties of earth-doped tellurite glass have affected many practical applications. Strong conversions of luminescence still pose a challenge to the research community [6]. The addition of different modifiers to the glass mixture will change the physical and optical characteristics of the glass. Significant attention has been given to lead oxide and zinc oxide modifiers due to their favourable effects on the density, thermal, and optical properties of glass [7]. However, to the best of our knowledge, there is very little research that has been carried out previously concerning the effect of the tellurite glass properties with different content of MgO and $MgCl_2$ modifiers. Hence, the influence of MgO and $MgCl_2$ in modifying the glass's structure and either improving or deteriorating the glass's physical and optical properties remains unclear. Therefore, this motivation reflects the necessity in investigating the effects of oxygen and chloride ions in MgO and $MgCl_2$ modifiers on the structural and optical properties of magnesium tellurite glass with the addition of samarium ions. In this work, two series of tellurite glass were synthesized with the incorporation of MgO and $MgCl_2$ by using the melt-quenching technique. The compatibility of the synthesized glass samples with different magnesium modifiers were evaluated based on their structural and optical properties to investigate their potential to be utilized in optical devices.

2. MATERIALS AND METHODS

2.1 Glass preparation

The glass samples with compositions $(79–x)TeO_2–xMgO–20Li_2O–1Sm_2O_3$ (Series 1) and $(79–x)TeO_2–xMgCl_2–20Li_2O–1Sm_2O_3$ (Series 2) with $0 \leq x \leq 15$ mol% were prepared using the melt-quenching technique. Starting raw materials of TeO_2 (99.99%), MgO (99.99%), Li_2O (99.99%), and Sm_2O_3 (99.99%) were weighed and mixed with a total weight of 5 g for each series for 30 minutes to ensure the homogeneity of the mixture during the mixing process. The mixtures were melted in an ambient air atmosphere in an alumina crucible at a temperature of 900 °C for 40 minutes. Then, the molten material was annealed to room temperature to remove thermal strains. Table 1 shows the nominal composition of the Series 1 and Series 2 prepared glass. In the end, two different series of magnesium tellurite glass were obtained, one using MgO as a modifier and the other using $MgCl_2$.

Table 1 Nominal composition of prepared glass

Series	Sample Name	Nominal composition (mol%)				
		TeO_2	MgO	$MgCl_2$	Li_2O	Sm_2O_3
1	TeO-MgO 0%	79	0		20	1
	TeO-MgO 5%	74	5		20	1
	TeO-MgO 10%	69	10		20	1
	TeO-MgO 15%	64	15		20	1
2	TeO-$MgCl_2$ 0%	79		0	20	1
	TeO-$MgCl_2$ 5%	74		5	20	1
	TeO-$MgCl_2$ 10%	69		10	20	1
	TeO-$MgCl_2$ 15%	64		15	20	1

2.2 Samples Characterization

The glass amorphous composition ranges of 0, 5, 10, and 15 mol% MgO and $MgCl_2$ were tested, and the crystalline phase was confirmed by X-ray diffraction (XRD) measurements using Rigaku Miniflex, with a monochromatic graphite for Cu-Kα radiation with λ = 1.5406 Å and with a power source of 40 keV and 25 mA. The density of the glass was investigated based on the Archimedes principle, in which deionized water was used as an immersion medium. By measuring the weight of samples in the air, w_{air} and in the water, w_{water} using an analytical balance, the density, ρ and molar volume, V_m of the glass samples were calculated using the following equation:

$$\rho_{glass} = \frac{w_{air}}{w_{water}} \rho_{water} \quad (1)$$

$$V_m = \frac{M_{glass}}{\rho_{glass}} \quad (2)$$

where M is the molar weight of the sample.

The basic and functional fractions of crystalline and non-crystalline matrices in the samples were determined using a Perkin Elmer Paragon 500 spectrometer with a spectra resolution of 4.0. The KBr pellet technique was used, in which a small amount of grounded glass was mixed with KBr and compressed at 5 tons of pressure to form a pellet. A pellet of KBr powder was compressed under the same conditions and under the same circumstances as the samples under testing, to be used as a reference sample.

The absorption spectra of powders from two series of tellurite glass were recorded at ambient temperature using a Perkin Elmer Lambda 950 with a wavelength range of 200 – 1400 nm. Powders cell was used to hold the powdered glass against the reflectance port of the internal UV-Vis, and barium sulphate ($BaSO_4$) was used as a background.

Edinburgh Instruments NIR 300/2 PL spectroscopy was used to speculate on the range of absorbed and reflected wavelengths of the glass. Photon emission spectra of glasses with an excitation wavelength of 413 nm were recorded, which utilize a high-quality diffraction grating for high dispersion and excellent imaging quality.

3. RESULTS AND DISCUSSION

3.1 X-ray diffraction (XRD)

Figure 1 presents the X-ray diffraction pattern of Series 1 and Series 2 with 0, 10, and 15 mol% amounts of MgO and $MgCl_2$ content, respectively. A broad halo peak was seen on the graph at a lower angle (20–40°), which is indicative of an amorphous structure. The intensity of the $TeOMgCl_2$ 0% glass sample is quite high compared to the glasses containing MgO and $MgCl_2$. This indicates the existence of a non-crystalline phase in the glass system. Besides, it is also proven that the glasses all experienced rapid cooling and had a limited time for atom arrangement. The amorphous phase of the glass structure was shown in the area underneath the graph. In comparison to the smaller region, the large area under the graph that represents the glass system is highly amorphous. This indicates that the presence of MgO and $MgCl_2$ reduces the amorphous properties of the glass system **Error! Reference source not found.**.

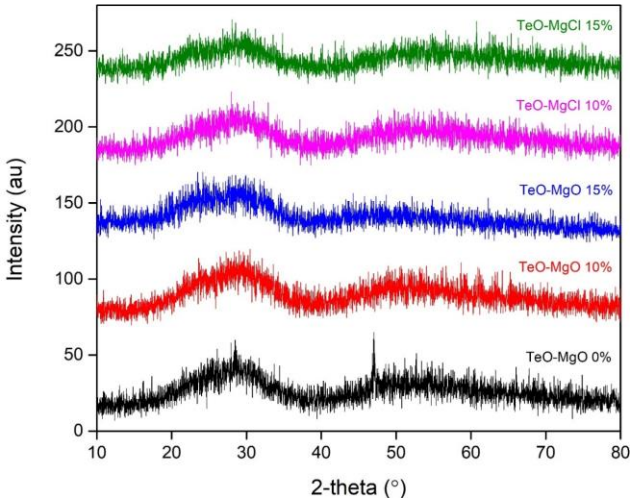

Figure 1. X-ray diffraction pattern of tellurite glass with different magnesium content

3.2 Density

Table 2 summarises the acquired physical characteristics of density (ρ) and molar volume (Vm) of the quaternary magnesium tellurite glass samples. The TeO_2 concentration in the examined glass composition was in the ranged from 79 to 64 mol%, whereas the amounts of MgO and $MgCl_2$ ranging from 5 to 15 mol%, and Li_2O and Sm_2O_3 are 20 and 1 mol%, respectively. Ternary glass TeO-MgO 0% has a measured density of 4.45 g/cm^3. It is worth noting that the addition of 5 mol% MgO and $MgCl_2$ resulted in a decrease in glass density of 4.45 g/cm^3 and 4.41 g/cm^3, respectively. In this scenario, the addition of a component with a higher molecular weight, TeO_2 (159.6 g/mol), with a lower molecular weight substance, MgO (40.30 g/mol) and $MgCl_2$ (95.21 g/mol), results in a drop in total molecular weight. The change in density is consistent with the findings obtained in other studies with a different component of tellurite glasses [9].

Further increases in MgO and $MgCl_2$ content led to an increase in density from 4.34 to 5.18 g/cm^3 and 4.41 to 4.98 g/cm^3, respectively. This is due to the amorphous network structural modifications, in which as MgO and $MgCl_2$ are added to the glass, additional cross-linked Te-O-Mg bonds are formed, increasing the network's cross-linking [10]. The rigidity of the glass structure increases as density increases. This would correspond to a rise in oxygen bridging in the glass

network [11]. At 10 and 15 mol%, tellurite glass with MgO modifier has a higher density than $MgCl_2$ glass, which indicates a higher glass network. The molar volume is proportional to the molecular weight but inversely related to density; thus, raising the molar volume causes the free volume to increase. The lower values of molar volume, indicate that the glass structure is densely packed [11]. In this case, as the modifier content increases, the molar volume decreases from 29.84 to 22.69 cm^3/mol for MgO and 30.03 to 25.29 cm^3/mol for $MgCl_2$ modifier. TeO–MgO 15% has the lowest molar volume with the highest density, which is expected to improve the stiffness and thermal stability of the glass.

Table 2 Molar weight, density (ρ) and molar volume (Vm) of prepared glass

Series	Sample name	Molar weight g/mol	Density, (ρ) g/cm^3	Molar volume, (Vm) cm^3/mol
1	TeO-MgO 0%	135.55	4.45	30.46
	TeO-MgO 5%	129.58	4.34	29.84
	TeO-MgO 10%	123.62	5.15	23.99
	TeO-MgO 15%	117.65	5.18	22.69
2	TeO-$MgCl_2$ 0%	135.55	4.45	30.46
	TeO-$MgCl_2$ 5%	132.33	4.41	30.03
	TeO-$MgCl_2$ 10%	129.11	4.44	29.11
	TeO-$MgCl_2$ 15%	125.89	4.98	25.29

3.3 Fourier-transform infrared spectroscopy (FTIR)

TeO_2-based glasses have TeO_4 (tbp), TeO_{3+1} polyhedra, and TeO_3 (tp) units in their structure [12]. According to Barney et al. (2013), the crystalline form of α-TeO_2 has only Te^{4+} in tetrahedral coordination with oxygen, but the pure amorphous TeO_2 structure has lower coordination than 4 [13]. Tellurium lone pair electrons have a high degree of polarizability; thus, the addition of a modifier to the tellurite glass causes the axial Te–O bonds to rupture and non-bridging TeO bonds to form [10]. Figure 2 shows the FTIR transmission spectra of Series 1 (TeO–MgO) and Series 2 (TeO–$MgCl_2$). Both series' spectra are quite similar. It should be emphasised, however, that the transmission intensity has been seen to vary with composition. Vibrational frequencies in Series 1 samples are 3414.53, 1640.52, 733.53, 528.77, and 460.79 cm^{-1}, whereas for Series 2 samples, the vibrational frequencies are 3412.93, 1638.12, 727.93, 519.97, and 460.79 cm^{-1}.

Strong and broad bands in the IR spectrum at 3414.53 cm^{-1} for Series 1 and 3412.93 cm^{-1} for Series 2; and a weak band at 1640.52 cm^{-1} for Series 1 and 1638.12 cm^{-1} for Series 2 are predicted for hydrated molecules in the lattice. This ascribes to the stretching and bending modes of the water molecule, respectively [14]. The broadening of the band is due to the disordered glass structure. According to Saddeek et al. (2008), the Te-O-Te vibrations for TeO_4 and TeO_3 groups are connected to the bands at 600–500 cm^{-1} and 650–750 cm^{-1}, respectively [15]. The IR spectra of the studied samples showed a shoulder near 733.53 cm^{-1} for Series 1 and 727.93 cm^{-1} for Series 2, and two well-resolved bands with a maximum around 528.77 cm^{-1} for Series 1, 519.97cm^{-1} for Series 2, and 460.79 cm^{-1} for both series. The formations of TeO_3 groups in the IR spectra are presented at the range of 733.53 cm^{-1} and 727.93 cm^{-1} for Series 1 and 2 respectively. The band at 528.77 cm^{-1} and 519.97cm^{-1} is identified in every spectrum and is assigned to TeO_4 structural unit vibrations, which contribute to the formation of bridging Te–O–Te bonds. By concentrating on the modification, the stretching vibrations of TeO_4 and TeO_3 change towards 528.77 cm^{-1} to 733.53 cm^{-1}, and 519.97 cm^{-1} to 727.93 cm^{-1}, respectively. The change in transmission bands is ascribed to TeO_4 group deformation into TeO_3 through TeO_{3+1} intermediate coordinate creation [16]. Magnesium (Mg) tetrahedral coordination in [MgO_4] is evidenced by vibrations ranging from 300 to 600 cm^{-1}

and 850 to 1200 cm^{-1} [17]. The characteristic absorption band at 460.79 cm^{-1} of TeO–MgO 15% could be credited to MgO_4 stretching vibration in cordierite [18]. The intensive band around 460.79 cm^{-1} for Series 2 which centred at TeO–$MgCl_2$ 15% is most likely due to the vibrations of opposed bonding formed, such as Cl-Mg-Cl bonds. After comparing the IR spectra, the glass network could be thought of as a combination of [TeO_4], [TeO_3] and [$MgCl_2$] and [MgO_4].

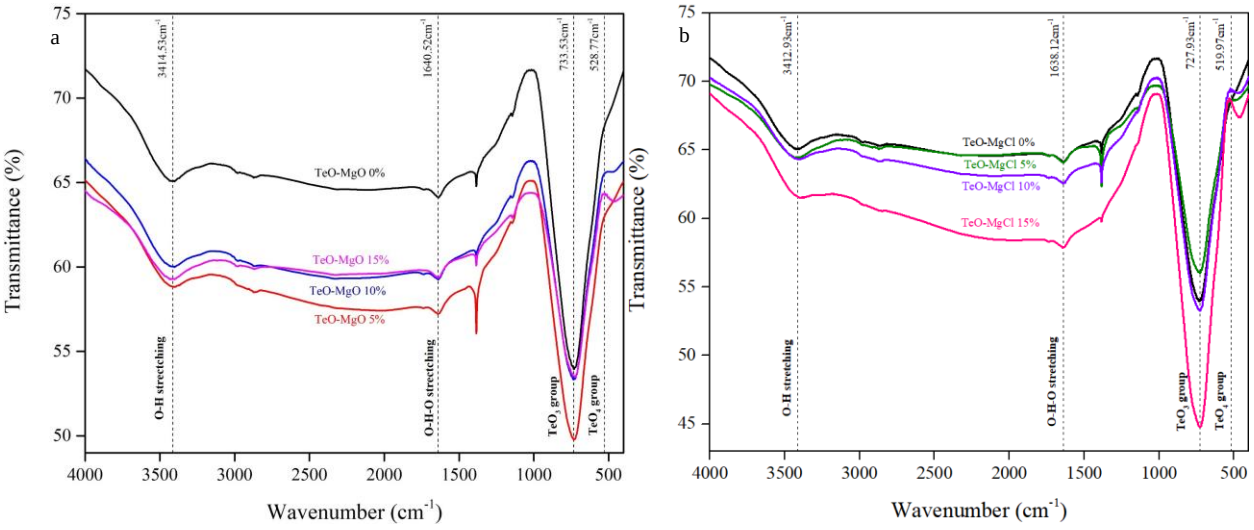

Figure 2. IR spectra of a) Series 1 b) Series 2

3.4 Ultraviolet–visible spectroscopy (UV-Vis)

The fluctuation of the optical absorption spectrum of magnesium tellurite glasses doped with 1 mol% Sm^{3+} ions in the 250–500 nm regions is seen in Figure 3. The absorption spectrum with no sharp edges explained the non-crystalline phase of the generated glasses [19]. The absorption spectra include the proportion of bands emanating from the ground state to the number of excited states of Sm^{3+} ions in the tellurite glass. According to Figure 3, the spectrum obtained for each composition exhibits the same features as the intensity changes. As a result, absorption bands were found at 285.71, 404.69, 420.41, and 475.73 nm for Series 1 and 285.71, 404.69, 420.18, and 474.62 nm for Series 2. These bands are made up of increases in atomic transition in linewidth caused by the existence of crystal structure refinement and the overlapping of Sm^{3+} ions' 4f orbitals with oxygens [20]. It is reported that, the optical properties of tellurite glass strongly depend on the composition [21].

The calculated optical band gap (E_g) for the indirect transition is shown in Table 3. The indirect optical band gap is calculated by extrapolating the curves' linear region to $(\alpha h\nu)^{1/2}$. The value of the optical band gap for pure TeO_2 glass is 3.79 eV [10]. As seen in Table 3, Series 1 constantly decreases from 3.42 to 3.36 eV for indirect bandgap with increasing of MgO content. It is agreeable that the decreasing value in E_g is due to the structural changes in the tellurite glass. The presence of MgO would destabilise the regular structure of the tellurite glass networks. The increment in the density of nonbridging oxygen causes the degree of crystallinity to become more haphazard [22]. Meanwhile, as for Series 2, the indirect optical band gap decreases at content 0-10 mol% of $MgCl_2$ (3.42–3.30 eV) but increase at 15 mol% at 3.40 eV for indirect optical band gap. According to the findings, the decreasing E_g value may be attributed to the assimilation of a limited

amount of dopants in the form of electron donor-acceptor (EDA) in the host lattice. By adding charges to the lattice, these EDA increase the specific conductance, resulting in a reduction in energy [23]. The E_g value is larger at high $MgCl_2$ 15 mol% content, and Cl^- participates in the amorphous network via charge transfer contact with more Te–O bands, which have a less ionic nature. In comparison to samples with $MgCl_2$ concentrations of 5 and 10 mol%, the electron-donating impact of $MgCl_2$ on the more electronegative Te–O strengthened the coordination, resulting in an improved glass connection.

Generally, the values of the optical energy band gap for tellurite glass range from 3.19 to 3.48 cm^3/mol. Thus, the current investigation findings of TeO–MgO and TeO–MgCl glass systems are likely relevant for optical applications.

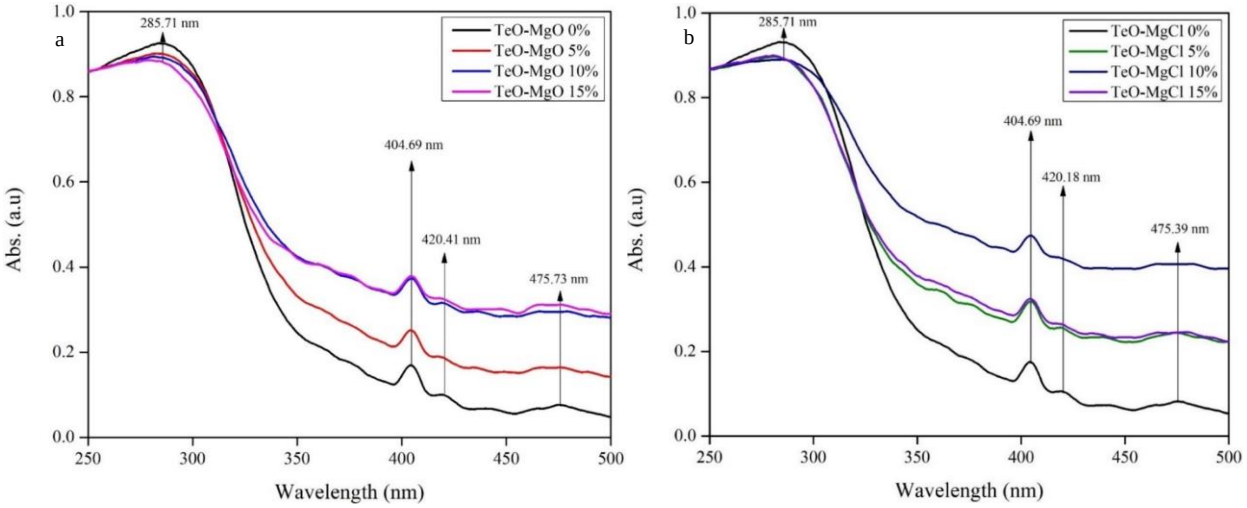

Figure 3. UV-Vis absorbance spectra for a) Series 1 b) Series 2

Table 3 Indirect optical band gap of prepared glass

Series	Sample Name	Indirect optical band gap, *Eg*, I (eV)
1	TeO-MgO 0%	3.42
	TeO-MgO 5%	3.39
	TeO-MgO 10%	3.37
	TeO-MgO 15%	3.36
2	TeO-$MgCl_2$ 0%	3.42
	TeO-$MgCl_2$ 5%	3.39
	TeO-$MgCl_2$ 10%	3.30
	TeO-$MgCl_2$ 15%	3.40

3.5 Photoluminescence spectroscopy (PL)

Figure 4 depicts the visible down-conversion luminescence spectra of Series 1 and Series 2, respectively. The emission spectra were collected at room temperature using wavelengths of 413 nm as excitation. For both glass series, the emission spectra show four emission bands centered at 562.54 nm, 599.14 nm, 645.97 nm, and 708.40 nm, which are ascribed to $^4G_{5/2} - {}^6H_{5/2}$, $^6H_{7/2}$, $^6H_{9/2}$, and $^6H_{11/2}$, respectively. The comparatively greater absorption in transition bands from

562.54 nm to 599.14 nm is greater than in other transition bands, while the absorption in transition bands from 562.54 to 708.40 nm is mild, which is consistent with prior studies. At 599.14 nm, a strong peak corresponding to reddish-orange emission from $^4G_{5/2} - {}^6H_{7/2}$ are observed [24]. In nature, the emission transitions of Sm^{3+} for $^4G_{5/2} - {}^6H_{5/2}$ and $^4G_{5/2}{}^- {}^6H_{7/2}$ are solely electric dipoles, whereas transitions $^4G_{5/2} - {}^6H_{9/2}$ and $^4G_{5/2} - {}^6H_{11/2}$ contain have both electric and magnetic contributions [25]. The observed emission spectrum of the tellurite glass demonstrates the existence of the trivalent state of samarium, which results in a high luminescence efficacy. Possible mechanisms for the excitation and emission spectra are depicted in the partial energy level diagram of the samarium ion, as shown in Figure 5. From the ground state absorption of $^6H_{5/2}$, the 413 nm excitation laser wavelength excites the Sm^{3+} ion to the high energy level $^4I_{9/2}$, and there is non-radiative relaxation to the $^4G_{5/2}$ energy level occurred. It is because any excitation above $^4G_{5/2}$ will quickly relax non-radiatively to $^4G_{5/2}$ energy level due to the narrow energy gaps between them [26]. Then, the emission takes place from the $^4G_{5/2}$ energy level to the lower energy levels. The radiative relaxation takes place at certain energy levels in the visible region revealed yellow, orange, and red emission bands in all glasses corresponding to the $^4G_{5/2} \rightarrow {}^6H_{5/2}$, $^4G_{5/2} \rightarrow {}^6H_{7/2}$, $^4G_{5/2} \rightarrow {}^6H_{9/2}$ and $^4G_{5/2} \rightarrow {}^6H_{11/2}$ transitions, respectively [27].

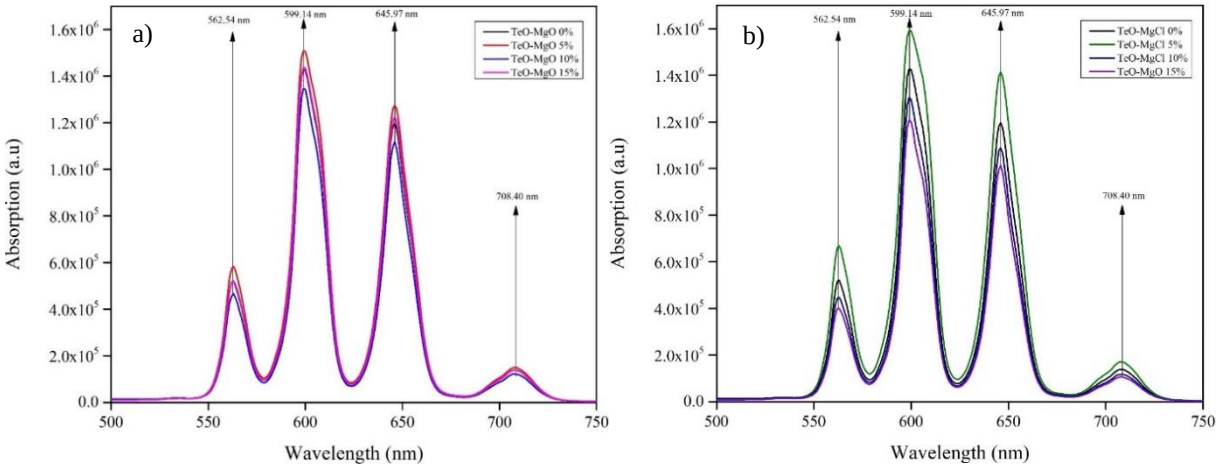

Figure 4. Photoluminescence spectra of Sm^{3+} doped a) Series 1 b) Series 2

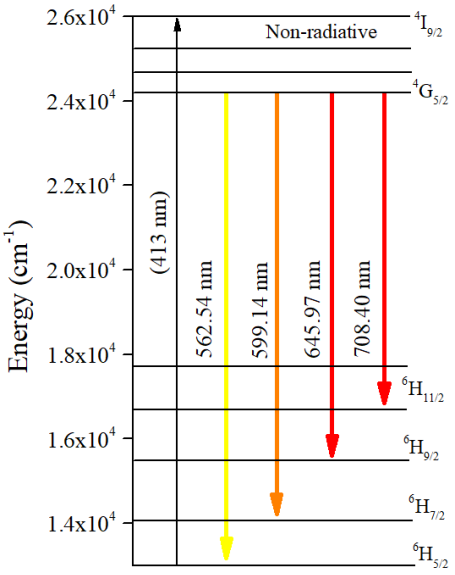

Figure 5. Partial energy level of Sm^{3+}

4. CONCLUSION

In this research, two series of tellurite glass, $(79–x)TeO_2–xMgO–20Li_2O–1Sm_2O_3$ (Series 1) and $(79–x)TeO_2–xMgCl_2–20Li_2O–1Sm_2O_3$ (Series 2) were successfully synthesized by using the melt-quenching technique. X-ray diffraction (XRD) measurements confirmed the amorphous nature of the glasses system. The glass density and molar density for Series 1 were found to be in the range of (4.45–5.18) g/cm^3 and (30.46–22.69) cm^3/mol, respectively. Meanwhile, for Series 2, the glass density is (4.45–4.98) g/cm^3 and the molar volume is in the range of 30.46–25.29 cm^3/mol. FTIR analysis revealed the existence of TeO_4 structural units as well as TeO_3 and $MgCl_2$ in Series 2 and MgO_4 in Series 1. The documented UV-Vis absorption spectrum contains four absorption bands centered at 285.71 nm, 404.69 nm, 420.41 nm, and 475.73 nm for Series 1 and 285.71 nm, 404.69 nm, 420.18 nm, and 474.62 nm for Series 2. Meanwhile, the indirect optical band gap for Series 1 is around (3.42–3.36 eV), whereas for Series 2 the indirect optical band gap is around (3.42–3.30 eV). By using an excited wavelength of 413 nm, four distinct bands could be seen in the photoluminescence spectrum, which was 562.54, 599.14, 645.97, and 708.40 nm which are assigned to the transitions of $^4G_{5/2}$ – $^6H_{5/2}$, $^6H_{7/2}$, $^6H_{9/2}$, and $^6H_{11/2}$ respectively. Similar studies with various oxychloride glasses revealed that the current glasses could be a viable candidate for optical devices. All in all, the optimum composition of glass is at TeO-MgO 15%, which exhibits the highest density and lowest molar volume and is good for drawing optical fibers. Since the refraction index is directly proportional to the molar refractivity, it is obvious that a glass composed of ions with similar polarizabilities will have a higher refractive index if the molar volume is small. A higher refractive index material can bend light more and allow the lens profile to be lower.

ACKNOWLEDGEMENTS

The authors would like to acknowledge the financial support from the Ministry of Higher Education under the Fundamental Research Grant Scheme (FRGS) No. FRGS/1/2021/TK0/UMP/02/54 (Vote No. RDU210152) and additional financial support under IIUM-UMP-UiTM Sustainable Research Collaboration Grant (Ref. No. IIUM/504/G/14/3/1/1/SRCG20-0007) (Vote No. RDU200715).

REFERENCES

[1] Tellurite. (2021). Retrieved from Mindat.org: https://www.mindat.org/min-3905.html
[2] Thomas, P. A. J. Phys. C: Solid State Phys. vol **21** issue 25 (1988) pp. 4611–4627.
[3] Ersundu, A. E., Karaduman, G., Çelikbilek, M., Solak, N., Aydın, S. J. Alloys Compd. vol **508** issue 2 (2010) pp. 266–272.
[4] Chen, D.D., Liu, Y.H., Zhang, Q.Y., Deng, Z. D., Jiang, Z. H. Mater. Chem. Phys. vol **90** issue 1 (2005) pp. 78–82.
[5] Grayson Krista (2019). Glass 101: Glass Formers – The Backbone of Glass. Mo-Sci Corporation.
[6] Jackson, C.T., Jeong, S., Dorlhiac, G. F., Landry, M. P. IScience, vol **24** issue 3 (2021) pp. 102156.
[7] Sidek, H.A.A., Elazoumi, S.H., El-Mallawany, R., Zaid, M.H.M., Matori, K.A., Halimah, M.K. J. Non-Cryst. Sol. vol **523** (2019) pp. 119640.
[8] Zalamin, S. N. F., Zaid, M. H. M., Matori, K. A., Karim, M. K. A., Yusof, N. N., Iskandar, S. M., Hisam, R., & Azlan, M. N. Optical Materials. vol **138** (2023) pp. 113653.
[9] Gayathri Pavani, P., Sadhana, K., Chandra Mouli, V. Phys. Rev. B Condens. Matter. vol. **406** issue 6-7 (2011) pp. 1242–1247.
[10] Bachvarova-Nedelcheva, A., Iordanova, R., Ganev, S., Dimitriev, Y. J. Non-Crys. Sol. vol **503–504** issue August 2018 (2019) pp. 224–231.
[11] Sahar, M. R., Yusoff, N. M. Mater. Today: Proc. vol **2** issue 10 (2015) pp. 5117-5121.
[12] Sekiya, T., Mochida, N., Soejima, A. J. Non-Cryst. Sol. vol **191** issue 1–2 (1995) pp. 115–123.
[13] E.R. Barney, A.C. Hannon, D. Holland, N. Umesaki, M. Tatsumisago, R.G. Orman, S. Feller. J. Phys. Chem. Lett. vol **4** issue 14 (2013) pp. 2312-2316.
[14] Golovnev, N. N., Molokeev, M. S., Sterkhova, I. V., Goryunov, Y. V., Atuchin, V.V. J. Mol. Struct. vol **1102** (2015) pp. 101–107.
[15] Saddeek, Y.B., Shaaban, E.R., Abdel-Rahim, F.M., Mahmoud, K.H. Phil. Mag. vol **88** issue 25 (2008) pp. 3059-3073.
[16] Ahmed M.M., Holland, D. Mater. Sci. Forum. vol **5** (1985) pp. 175-184.
[17] Gautam, C., Yadav, A.K., Singh, A.K. Int. Sch. Res. Notices. vol **2012** (2012) pp. 1– 17.
[18] Deng, L., Fu, Z., Mingxing, Z., Li, H., Yao, B., He, J., Ma, Y. J. Non-Cryst. Solids. vol **575** (2022) pp. 121217.
[19] Zalamin, S. N.F., Zaid, M. H.M., Matori, K.A., Karim, M.K.A., Yamin, N.A.M., Ismail, N.A.N. J. Phys. Chem. Sol. vol **163** (2022) pp. 110563.
[20] Lakshmi, Y.A., Swapna, K., Mahamuda, S.K., Venkateswarlu, M., Rao, A.S. Solid State Sci. vol **116** (2021) pp. 106609.

[21] El-Mallawany, R., Abdalla, M.D., Ahmed, I.A. Mater. Chem. Phys. vol **109** issue 2–3 (2008) pp. 291–296.
[22] Effendy, N., Sidek, H.A.A., Halimah, M.K., Zaid, M.H.M. Mater. Chem.Phys. vol **273** (2021) pp. 125156.
[23] Kramadhati, S., Thyagarajan, K. Int. J. Eng. Res. Dev. vol **6** issue 8 (2013) pp. 15-18.
[24] Babu, A.M., Jamalaiah, B.C., Suhasini, T., Srinivasa, R.T. Rama, M.L. Solid State Sci. vol **13** (2011) pp. 574-578.
[25] Aziz, S.M., Umar, R., Yusoff, N.M., Rosid, S.J.M., Amin, S.N.S.M. Int. J. Sci. Tech. Res. vol **8** issue 9 (2019) pp. 1976–1980.
[26] Busra, N.A.N., Arifin, R., Ghoshal, S.K., Nazlan, R. Mater. Sci. Forum. vol **981** (2020) pp. 73-77.
[27] Ravi, O., Madhukar Reddy, C., Manoj, L., Deva Prasad Raju, B. J. Mol. Struct. **vol** 1029 (2012) pp 53-59.